ARTICLES

Journal of Semiconductors
(2019) 40, 052501
doi: 10.1088/1674-4926/40/5/052501

Magneto-transport properties of the off-stoichiometric Co_2MnAl film epitaxially grown on GaAs (001)

Zhifeng Yu[1, 2], Hailong Wang[1, 2], Jialin Ma[1, 2], Shucheng Tong[1, 2], and Jianhua Zhao[1, 2, †]

[1]State Key Laboratory of Superlattices and Microstructures, Institute of Semiconductors, Chinese Academy of Sciences, Beijing 100083, China
[2]Center of Materials Science and Optoelectronics Engineering, University of Chinese Academy of Sciences, Beijing 100190, China

Abstract: We have investigated the magneto-transport properties of an off-stoichiometric full-Heusler alloy Co_2MnAl single-crystalline film. The $Co_{1.65}Mn_{1.35}Al$ (CMA) film epitaxially grown on III–V semiconductor GaAs substrate exhibits perpendicular magnetic anisotropy. The resistivity of the CMA film increases with the temperature T decreasing from 300 to 5 K, showing a semiconducting-like transport behavior. Different activation energies are found in three temperature regions with transition temperatures of 35 and 110 K. In the meanwhile, the remanent magnetization can be described by $T^{3/2}$ and T^2 laws in the corresponding medium and high T ranges, respectively. The transition at around 110 K could be attributed to the ferromagnetism evolving from localized to itinerant state. The Curie temperature of the CMA film is estimated to be ~640 K. The intrinsic anomalous Hall conductivity of ~55 $\Omega^{-1}cm^{-1}$ is obtained, which is almost twenty times smaller than that of Co_2MnAl.

Key words: full-Heusler alloy; magneto-transport property; activation model; molecular-beam epitaxy

Citation: Z F Yu, H L Wang, J L Ma, S C Tong, and J H Zhao, Magneto-transport properties of the off-stoichiometric Co_2MnAl film epitaxially grown on GaAs (001)[J]. *J. Semicond.*, 2019, 40(5), 052501. http://doi.org/10.1088/1674-4926/40/5/052501

1. Introduction

Heusler compounds have drawn much attention in recent years due to their high Curie temperature (T_C)[1, 2] and flexible tunability[3–6], making them complex and diversified, and thus bringing a lot of interesting phenomena[3]. Among these materials, Co–Mn–Al ternary Heusler alloy is an attractive system, especially in the cases of Co_2MnAl as a half-metal[7] and Mn_2CoAl as a typical spin gapless semiconductor[8–10]. The Fermi levels in both cases lie in the gaps of their minority-spin bands. But in their majority-spin bands, Co_2MnAl acts like a metal, while Mn_2CoAl is close to a zero-gap semiconductor[11] featuring a semiconducting-like transport behavior[8, 10].

Different from Co_2MnAl or Mn_2CoAl, we have synthesized $Co_{1.65}Mn_{1.35}Al$ (CMA), an off-stoichiometric alloy Co_2MnAl, in which perpendicular magnetic anisotropy (PMA) emerges as a result of residual strain. This material provides a material platform for studying the effect of strain on spin-orbit coupling related phenomena such as anomalous Hall effect (AHE), and could also be a promising candidate for potential applications in spintronic devices due to its PMA characteristic[12]. Therefore, it is meaningful to investigate the physical properties, especially the magneto-transport behavior of the CMA film systematically.

In this work, we report the temperature T dependence of the longitudinal resistivity ρ_{xx} and the negative magneto-resistance (MR) at different temperatures of a 20 nm-thick CMA film. The semiconducting-like transport character in the T range between 5 and 300 K implies the existence of an activation energy E_a. It is found that ρ_{xx} can be described by a simple activation model with varying E_a in different T regions. The T dependences of the magnetization M are also different correspondingly. The first transition temperature at around 110 K could be ascribed to a transition from localized to itinerant ferromagnetism. We measure the Hall resistivity at several temperatures and obtain the intrinsic anomalous Hall conductivity of ~55 $\Omega^{-1}cm^{-1}$, which is almost twenty times smaller than that of Co_2MnAl[13].

2. Experiments

The single-crystalline film of CMA was epitaxially grown on GaAs (001) substrate by molecular-beam epitaxy (MBE). After the GaAs de-oxidation and buffer layer deposition, a 20 nm-thick CMA film was grown at 200 °C, capped with 2 nm-thick aluminum for protection from oxidation. The sample was patterned to a standard Hall bar, with the channel along the GaAs [110] direction for transport measurements. The magnetic field H was applied perpendicular to the film plane, i.e., parallel with the GaAs [001] direction. The transport data of the film were collected with T between 5 and 300 K and H up to 50 kOe using a physical property measurement system (Quantum Design, PPMS-9). The magnetic properties of CMA film were measured using a superconducting quantum interference device (SQUID) down to 5 K.

3. Analyses and results

Fig. 1(a) shows the dependence of ρ_{xx} on T varying from 5 to 300 K with a zero magnetic field. ρ_{xx} increases with decreasing temperature in the whole range of T in our experiment. Different from Co_2MnAl[13], ρ_{xx} of the CMA film resembles that of Mn_2CoAl films following an activation-type dependence[8, 10], which is usually described by a simple activation model[10, 14]: $\sigma_{xx}(T) = 1/\rho_{xx}(T) = \sigma_0 + \sigma_a \exp(-E_a/k_BT)$, where σ_0 denotes the non-stoichiometric contributions at the low temperature and

Correspondence to: J H Zhao, jhzhao@red.semi.ac.cn
Received 22 APRIL 2019.

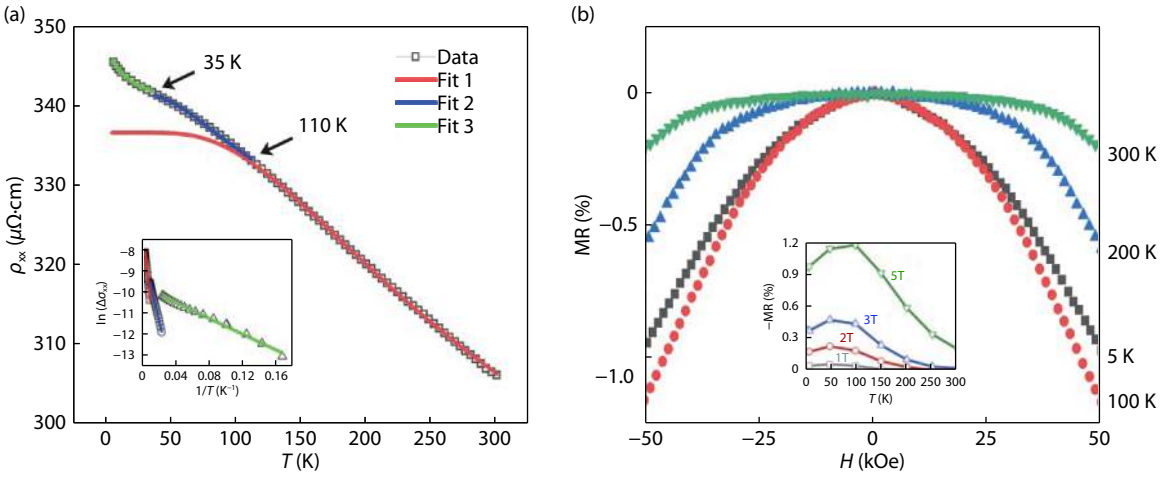

Fig. 1. (Color online) (a) T dependence of the zero-field ρ_{xx} varying from 5 to 300 K. The fitting curves using activation model in different T regions are plotted in red, blue and green lines, respectively. The inset gives a linear relation between $\ln(\Delta\sigma_{xx})$ and $1/T$ in the corresponding T ranges. (b) The MR at several selected temperatures. The inset shows the temperature dependence of MR at specific applied field.

σ_a is a coefficient with the same dimension as conductivity, respectively. As shown in Fig. 1(a), an obvious deviation from the fitting curve to $\rho_{xx}(T > 110$ K) is found at temperatures lower than 110 K, which could result from the change of the E_a in the equation. Thus we learn this transition between different T regions divided by the T points at 35 and 110 K. The best fits of the data yield the critical parameters of $E_{a1} = 34$ meV, $\sigma_{01} = 2.97 \times 10^{-3}$ $\mu\Omega^{-1}$cm^{-1} (110 to 300 K), $E_{a2} = 15$ meV, $\sigma_{02} = 2.93 \times 10^{-3}$ $\mu\Omega^{-1}$cm^{-1} (35 to 110 K), and $E_{a3} = 1.4$ meV, $\sigma_{03} = 2.89 \times 10^{-3}$ $\mu\Omega^{-1}$cm^{-1} (5 to 35 K), respectively. To clearly show the change of E_a, we plot the relations of $\ln(\Delta\sigma_{xx}) = \ln(\sigma_{xx} - \sigma_0)$ versus $1/T$ in the inset of Fig. 1(a), which depict good linear dependencies and different slopes in three T regions. According to these results, the CMA film is discovered to have a decreasing E_a when T is lowered, which could be attributed to a band shift with T.

The relations of MR with H are selectively presented in Fig. 1(b). The MR is defined as $(\rho_{xx} - \rho_{xx0})/\rho_{xx0} \times 100\%$, where $\rho_{xx0} = \rho_{xx}(H = 0)$. The negative MR is observed over the whole T range, which is usually ascribed to the spin-dependent scattering in similar systems[10, 15]. And it means that this scattering, which is inevitably affected by magnetism, dominates MR compared to the contributions of the cyclotron effect in our measurement with H lower than 50 kOe[16]. There are two major changes of MR with T and H, respectively. One is that MR ($T > 200$ K) clearly changes much more slowly than those at low temperatures when H is not larger than 30 kOe. This variation could be an evidence for different activation modes in different T regions, consistent with the implications from $\rho_{xx}(T)$. Another difference is that the MR approaches a linear trend when it reaches about 30 kOe and higher. This linear dependency between MR and H has been reported in the Mn_2CoAl and some other spin gapless systems[8, 17]. Moreover, the MR of the CMA film shows a maximum in the temperatures between 50 and 100 K as shown in the inset of Fig. 1(b). The maximum value of MR here could possibly result from the change of the band structure rather than the combined influence of the impurity and the spin-dependent scattering reported in Mn_2CoAl[8, 9].

In order to learn whether a similar transition happens for the ferromagnetism of this sample, we carried out the magnetic measurements using a SQUID magnetometer. The sample was cooled down to 5 K with $H = 0$ and then saturated by a magnetic field as high as 50 kOe. After H was set at 20 Oe, the T dependence of M along the [001] direction was measured by heating the sample from 5 to 280 K. The results are shown in Fig. 2(a). For our CMA film, a linear dependence of M^2 on T^2 is observed with T ranging from about 110 to 280 K, which is ordinary in itinerant ferromagnetic materials such as MnSi[18] and $ZrZn_2$[19]. Therefore, $M(T)$ can be fitted by the formula of $M(T) = M(0) \times [1 - (T/T_C)^2]^{1/2}$. The best fit yields the parameters of $M_1(0) = 292$ emu/cm^3 and $T_C = 640$ K, close to 693 K of Co_2MnAl[2] and 720 K of bulk Mn_2CoAl[8]. However, an obvious deviation from this T^2 behavior is observed when T is lower than 110 K. In the T range between 43 and 110 K, the more rapid variation of M versus T can be described by the classical Bloch $T^{3/2}$ law: $M(T) = M(0)(1 - \eta T^{3/2})$, where η is related to the spin-wave stiffness constant and exchange coupling energy. It means that the variation of $M(T)$ in this T range could be attributed to collective spin wave excitations[17]. The best fit of the curve yields the $M_2(0)$ and η values of 294 emu/cm^3 and 1.8×10^{-5} K$^{-3/2}$, respectively. Furthermore, an enhanced changing rate of the $M(T)$ curve occurs in the lowest T range between 5 and 35 K. Although the picture of this anomalous behavior is still unclear in our system, the $M(T)$ curve may be described by an exponential dependence: $M(T) = M(0)(1 - \alpha\exp(-\Delta/T))$, where the coefficients $\alpha = 1.64 \times 10^{-2}$ and $\Delta = 3.74 \times 10^{-2}$ K are obtained. To show the change of $M(T)$ near 110 K more clearly, the dependences of $\ln(1 - M(T)^2/M(0)^2)$ ($T \sim 110$–280 K) and $\ln(1 - M(T)/M(0))$ ($T \sim 43$–110 K) on T are plotted in Fig. 2(b), showing good linearity in both regions. Combining the above results of transport and magnetic measurements, the transition of ρ_{xx} and M could be originated from the same contributions because similar changes take place near 35 and 110 K.

Fig. 3(a) shows the measured Hall resistivity ρ_{xy} varying with H and T after the subtraction of the background signals coming from ρ_{xx}. ρ_{xy} is dominated by the anomalous Hall signal, which reflects the ferromagnetism corresponding to the

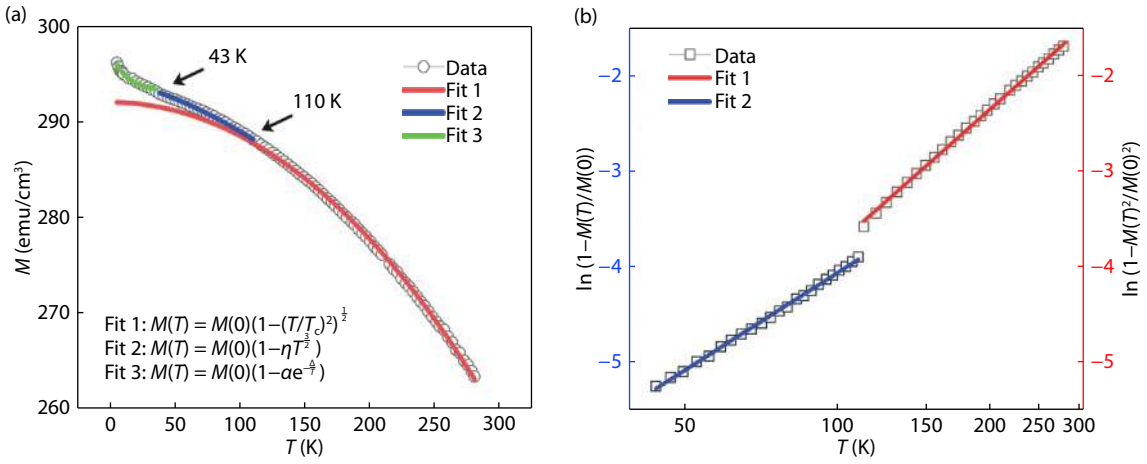

Fig. 2. (Color online) T dependence of M varying from 5 to 280 K. (a) The fitting curves using T^2, $T^{3/2}$ and exponential dependences in different T regions are plotted in red, blue and green lines, respectively. The formulas describing $M(T)$ in corresponding T regions are shown. (b) The linear relations of $\ln(1-M(T)^2/M(0)^2)$ (red line) and $\ln(1-M(T)/M(0))$ (blue line) versus T.

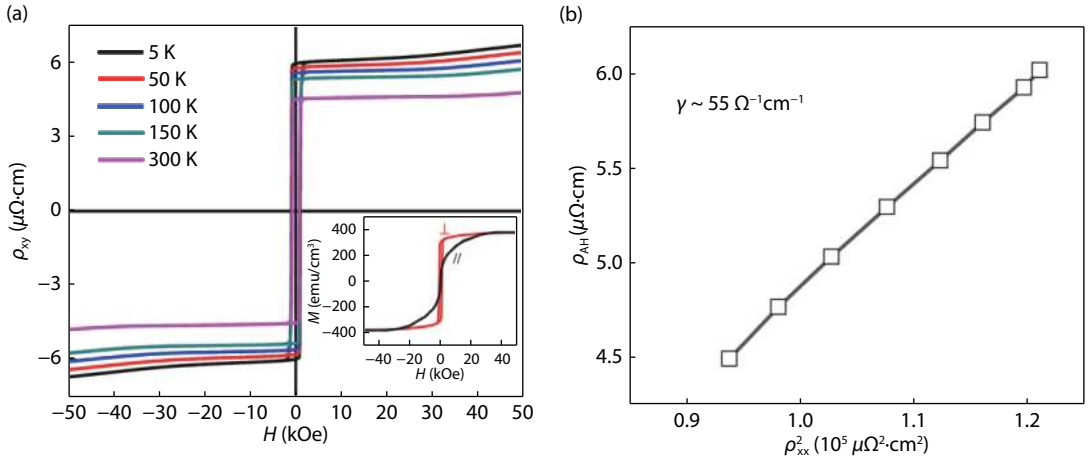

Fig. 3. (Color online) (a) $\rho_{xy}(H)$ varying with H and T after the subtraction of the background signals originated from ρ_{xx}. The inset shows the hysteresis loop at 5 K perpendicular and parallel to the film plane. (b) The relation between ρ_{AH} and ρ_{xx}^2. The slope value is estimated to be about 55 Ω^{-1}cm^{-1}.

hysteresis loop shown in the inset. The Hall resistivity is generally described by the formula: $\rho_{xy}(H) = R_oH + R_AM(H)$, where R_o and R_A are the ordinary and anomalous Hall coefficient, respectively. When H is large enough to saturate a ferromagnetic material, the slope of $\rho_{xy}(H)$ is mainly determined by $R_o = 1/(nq)$ based on the one band model, where n is the carrier concentration and q equals the charge of an electron. However, in the CMA film, we notice that the slope of $\rho_{xy}(H)$ gradually becomes larger when H is increased, which seems to be contradicted with the saturation state shown in the hysteresis loop. Considering the different behaviors of MR when H is lower and higher than 30 kOe, M could also change gradually with H which is not evident compared to the remanent magnetization. We then obtain ρ_{AH} as the value of $\rho_{xy}(H = 0)$ for estimating the anomalous Hall conductivity (AHC). In general, the anomalous Hall resistivity ρ_{AH} can be described in terms of ρ_{xx} in the form of $\rho_{AH} = \beta\rho_{xx} + \gamma\rho_{xx}^2$, where β characterizes the extrinsic skew scattering and γ denotes the intrinsic origin or the extrinsic side-jump scattering[20]. The ρ_{xx} and ρ_{xy} are measured simultaneously in our experiment and ρ_{AH} shows a linear dependence on ρ_{xx}^2 as shown in Fig. 3(b). The γ can be described by the slope value of ρ_{AH} versus ρ_{xx}^2, which is estimated to be ~55 Ω^{-1}cm^{-1} in favor of a topological origin from Berry phase effect in the case of ρ_{xx} ~ 300–350 $\mu\Omega$·cm[9, 20, 21]. Therefore, the intrinsic AHC of the CMA film is almost twenty times smaller than that of Co_2MnAl film[14] but relatively larger than that of bulk Mn_2CoAl[8].

4. Conclusion

In conclusion, we have systematically investigated the magneto-transport properties of a 20 nm-thick CMA film. The film exhibits semiconducting-like transport behavior below 300 K. Its longitudinal resistivity $\rho_{xx}(T)$ is properly described by a simple activation model with different activation energies in three T regions separated by 110 and 35 K. The activation energies are 34, 15 and 1.4 meV in the temperature range of 110–300, 35–110, and 5–35 K, respectively. Similar transitions at nearly the same temperature in $M(T)$ have also been discovered, implying a same origin of the transitions of $\rho_{xx}(T)$ and $M(T)$, which might probably be related to the bands' shift. The Curie temperature is estimated to be ~640 K, which is a typical value among full-Heusler alloys. An intrinsic AHC of about

55 $\Omega^{-1}cm^{-1}$ is obtained from the linear dependence of ρ_{AH} versus ρ_{xx}^2. Further experiments and calculations are needed to understand the relations between the transitions and the band structures of the film.

Acknowledgements

This work was supported by the Ministry of Science and Technology under Grant Nos. 2015CB921500, 2017YFB0405 701 and the National Natural Science Foundation of China under Grant Nos. U1632264 and 11704374.

References

[1] De Groot R A, Mueller F M, Van Engen P G, et al. New class of materials: half-metallic ferromagnets. Phys Rev Lett, 1983, 50(25), 2024

[2] Trudel S, Gaier O, Hamrle J, et al. Magnetic anisotropy, exchange and damping in cobalt-based full-Heusler compounds: an experimental review. J Phys D, 2010, 43(19), 193001

[3] Wollmann L, Nayak A K, Parkin S S P, et al. Heusler 4.0: tunable materials. Ann Rev Mater Res, 2017, 47, 247

[4] Nayak A K, Nicklas M, Chadov S, et al. Design of compensated ferrimagnetic Heusler alloys for giant tunable exchange bias. Nat Mater, 2015, 14(7), 679

[5] Gueye M, Wague B M, Zighem F, et al. Bending strain-tunable magnetic anisotropy in Co_2FeAl Heusler thin film on Kapton. Appl Phys Lett, 2014, 105(6), 062409

[6] Zhang B, Wang H L, Cao J, et al. Control of magnetic anisotropy in epitaxial Co_2MnAl thin films through piezo-voltage-induced strain. J Appl Phys, 2019, 125(8), 082503

[7] Picozzi S, Continenza A, Freeman A J. Co_2MnX (X= Si, Ge, Sn) Heusler compounds: An ab initio study of their structural, electronic, and magnetic properties at zero and elevated pressure. Phys Rev B, 2002, 66(9), 094421

[8] Ouardi S, Fecher G H, Felser C, et al. Realization of spin gapless semiconductors: The Heusler compound Mn_2CoAl. Phys Rev Lett, 2013, 110(10), 100401

[9] Jamer M E, Assaf B A, Devakul T, et al. Magnetic and transport properties of Mn_2CoAl oriented films. Appl Phys Lett, 2013, 103(14), 142403

[10] Xu G Z, Du Y, Zhang X M, et al. Magneto-transport properties of oriented Mn_2CoAl films sputtered on thermally oxidized Si substrates. Appl Phys Lett, 2014, 104(24), 242408

[11] Feng Y, Zhou T, Chen X, et al. The effect of Mn content on magnetism and half-metallicity of off-stoichiometric Co_2MnAl. JMMM, 2015, 387, 118

[12] Zhang X, Cheng Y, Zhao W, et al. Exploring potentials of perpendicular magnetic anisotropy stt-mram for cache design. IEEE International Conference on Solid-State and Integrated Circuit Technology (ICSICT), 2014, 1

[13] Meng K K, Miao J, Xu X, et al. Thickness dependence of magnetic anisotropy and intrinsic anomalous Hall effect in epitaxial Co_2MnAl film. Phys Lett A, 2017, 381(13), 1202

[14] Gofryk K, Kaczorowski D, Plackowski T, et al. Magnetic and transport properties of the rare-earth-based Heusler phases R Pd Z and R Pd 2 Z (Z= Sb, Bi). Phys Rev B, 2005, 72(9), 094409

[15] Raquet B, Viret M, Warin P, et al. Negative high field magnetoresistance in 3d ferromagnets. Physica B, 2001, 294, 102

[16] Hordequin C, Pierre J, Currat R. Magnetic excitations in the half-metallic NiMnSb ferromagnet: From Heisenberg-type to itinerant behaviour. JMMM, 1996, 162(1), 75

[17] Du Y, Xu G Z, Zhang X M, et al. Crossover of magnetoresistance in the zero-gap half-metallic Heusler alloy Fe_2CoSi . Europhys Lett, 2013, 103(3), 37011

[18] Ishikawa Y, Shirane G, Tarvin J A, et al. Magnetic excitations in the weak itinerant ferromagnet MnSi. Phys Rev B, 1977, 16(11), 4956

[19] Wohlfarth E P. Very weak itinerant ferromagnets application to $ZrZn_2$. J Appl Phys, 1968, 39(2), 106

[20] Nagaosa N, Sinova J, Onoda S, et al. Anomalous hall effect. Rev Modern Phys, 2010, 82(2), 1539

[21] Tian Y, Ye L, Jin X. Proper scaling of the anomalous Hall effect. Phys Rev Lett, 2009, 103(8), 087206